Electronic Supplementary Material (ESI) for Nanoscale.
This journal is © The Royal Society of Chemistry 2015

Supporting Information

Experimental Section

Poly(allylamine hydrochloride) (**1**; average M_w~17,500, product Nr. 283215) and poly(diallyldimethylammonium chloride) (**2**; average M_w <100,000, product Nr. 522376) were supplied by Sigma-Aldrich. Nanodiamonds were supplied by Microdiamant Switzerland (MSY 0-0.05). The nanodiamonds were treated with a mixture of HNO_3 and H_2SO_4 (85 °C, 3 days), washed with 0.1 M NaOH and 0.1 M HCl, washed five times with water, and freeze-dried. Purified nanodiamond powder (160 mg), containing approximately 100–200 ppm of natural nitrogen impurities, was pressed in an aluminium target holder and irradiated with a 15.5 MeV proton beam extracted from the isochronous cyclotron U-120M for 70 min (fluence $6 \times 10^{16}\ \mathrm{cm}^{-2}$). The irradiated material was annealed at 900 °C for 1 h and subsequently oxidized in the air for 6 h at 510 °C. The nanodiamonds were then treated by the same procedure as described above for starting material. Prior to use, the particles were dissolved in water (1 mg/mL) and sonicated with a probe (Cole-Parmer, 750 W) for 30 min. The resulting transparent colloid was filtered using a 0.2 μm PVDF microfilter.

Bright field TEM micrographs were recorded with a JEOL JEM-1011 electron microscope operated at 60 kV and equipped with a Veleta side mounted camera. Dynamic light scattering and zeta potential measurements were recorded with a Zetasizer Nano ZS system (Malvern Instruments) at room temperature. For zeta potential measurements, the ‘dip cell’ was used. Photoluminescence spectra were measured using a Renishaw InVia Raman Microscope; excitation wavelength 514 nm with 15 mW laser power, using x50 long infinity corrected distance objective. The measurements in aqueous solutions (1 mg/mL) were performed in a Hellma fluorescence cuvette (type no. 105.252-QS). Fluorescence images were taken using time-resolved fluorescence confocal microscope (MicroTime200 – PicoQuant), excitation wavelength 532 nm, 1.2 mW laser power, using 60x water immersion objective (Olympus). Used band-pass filters: 580/10nm (Edmund Optics, OD4) for NV^0 spectral region, 638/10nm (Edmund Optics, OD4) for NV^- spectral region. Figures represent area of 20x20 μm, taking 300x300px. Image processing was performed using Matlab (R2014b, Mathworks). NV^0/NV^- ZPL intensity ratio was calculated for selected pixels of fluorescence intensity matrixes representing NV^0 spectral region and NV^- spectral region. Pixel selection was performed using calculated fast fluorescence lifetime (FLIM) (>13 ns) and counts/pixel (>100 cts) thresholds. Calculated NV^0/NV^- ratios (red, blue, green) were superimposed on intensity image (gray colormap).

Sample preparation: An appropriate weight of each polymer (3.07 mg of **1** or 14.4 mg of **2**) was dissolved in 1 mL water to prepare stock solutions in which the concentration of monomeric unit was 31.2 mM.
For DLS and zeta potential measurements, FND stock solution (500 μL, 1 mg/mL), water (450 μL), and stock solution of the appropriate polymer (50 μL) were mixed together to achieve 1 mL of sample with final concentrations of 0.5 mg/mL FND and 1.56 mM polymer. The pH of each sample was adjusted with HCl or NaOH to the desired value. Zeta potential and size were measured after adjustment, and pH was checked after measurement. If the initial and end pH differed more than by 0.1 unit, the measurement was repeated.

For fluorescence measurements, aqueous solution of FND (2 mg/mL), water and solution of a polymer were mixed together to achieve 1 mL of sample with final concentration of 1 mg/mL FND and 3.12 mM polymer. The pH of each sample was adjusted with HCl or NaOH to the desired value. Samples were left to reach binding equilibrium overnight before measurements.

For fluorescence imaging, aqueous solution of FND (0.02 mg/mL) was deposited by dropcasting on acid-cleaned glass cover slide (thickness 0.17 μm). FNDs were fixed on the glass surface. To take a reference image (marked as FND; Fig. 3B and S5 – left), 20 μl droplet of DI water was placed on the surface (to avoid influence of variation of the refractive index on the fluorescence intensity after addition of a polymer diluted in water). 2 μl of 31.2 mM polymer 2 or was added to the droplet and left to settle for 10 minutes before measurement.

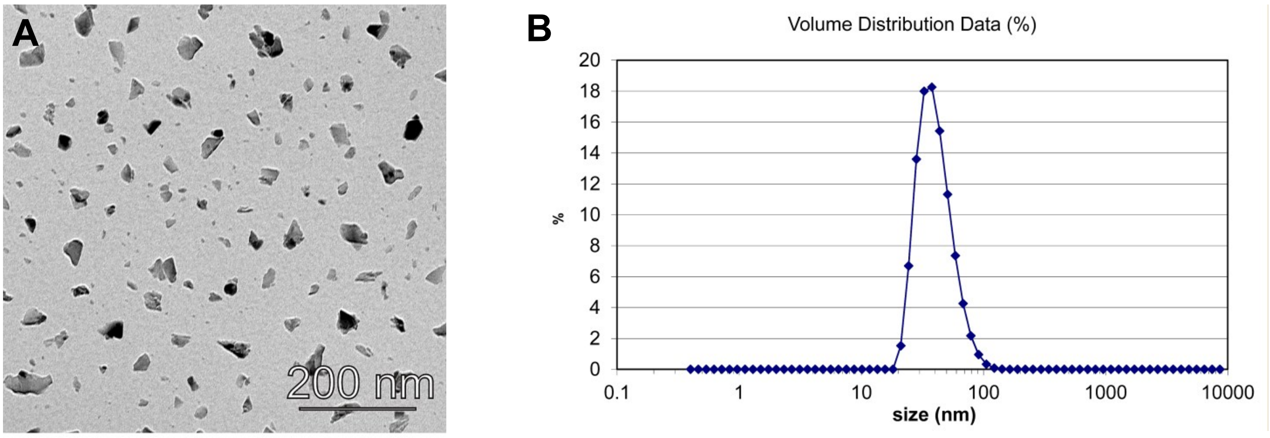

Figure S1: A) TEM micrographs of HPHT FNDs on carbon-coated grid. Mean equivalent diameter of the particles is 14 nm. B) Size distribution histogram of FNDs obtained from dynamic light scattering. The Z-average diameter is 49 nm.

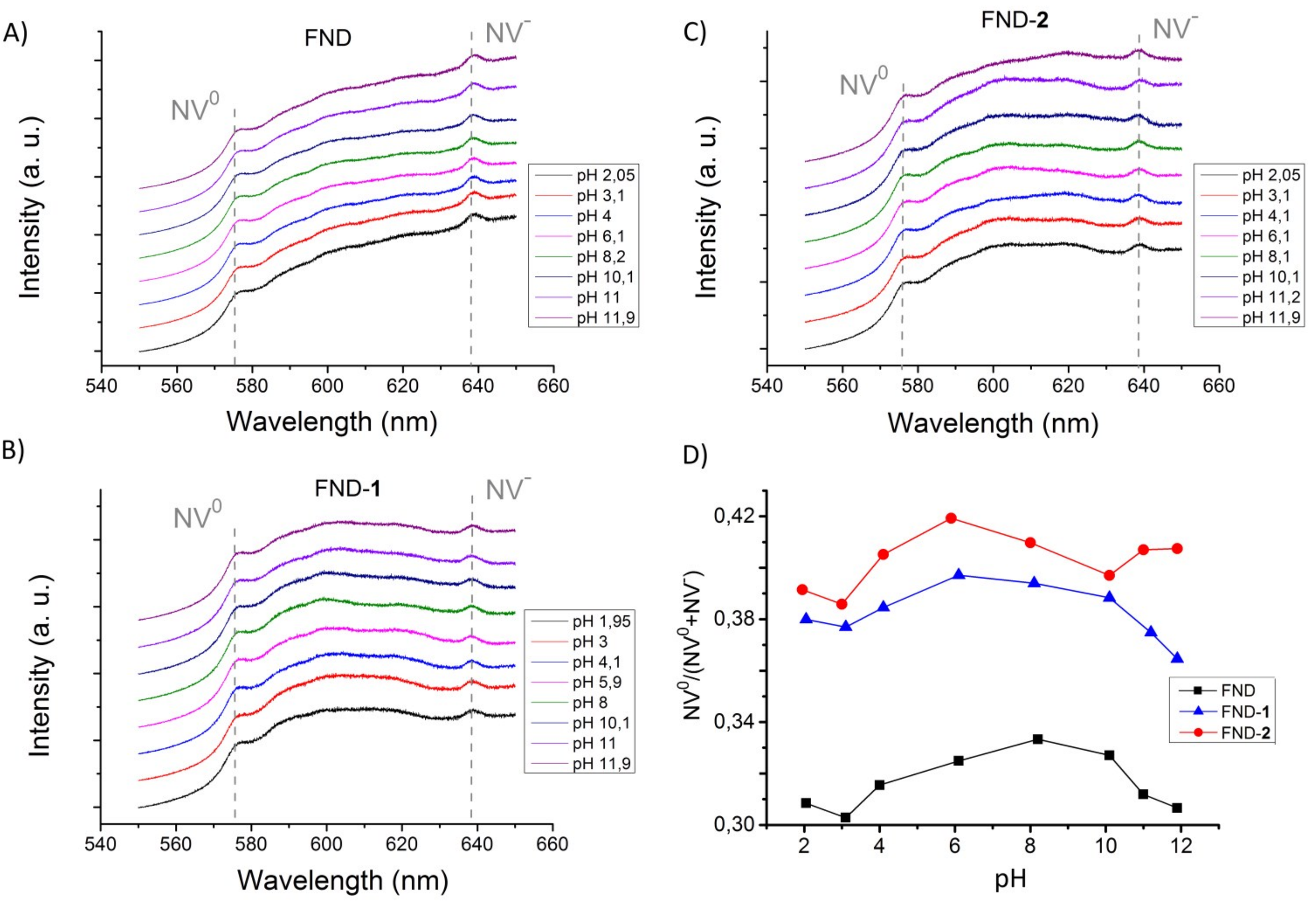

Figure S2: Section of fluorescence spectra involving ZPL of the NV^0 and NV^- states for A) FND and complexes B) FND-**1** and C) FND-**2** measured at various pH. Each spectrum is normalized to the NV^0 ZPL. For clarity, spectra in each graph are shifted along the y-axis. D) Dependence of surface-charge-induced modulation of fluorescence on pH for FND-**1** and FND-**2** complexes related to unmodified FND. The changes are expressed as the emission ratio and calculated from maximum intensity of NV^0 and NV^- ZPL peak in fluorescence spectra. Note the significant difference between FND and each of FND-**1** and FND-**2**. The differences between complexes FND-**1** and FND-**2** are, however, not significant even in the alkaline region.

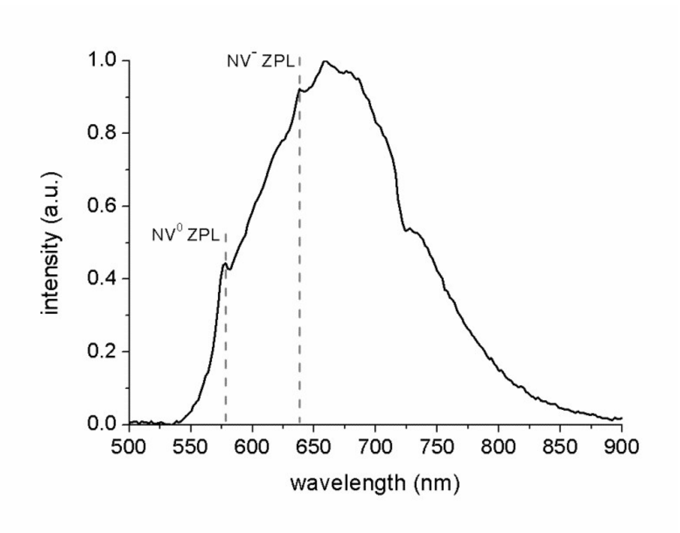

Figure S3: Example of fluorescence spectrum of FND measured with a fluorescence spectrometer according to ref. [3]. This setup is different than Raman setup used in Figures 3, S2 and S4 and enables recording of full range spectra including the phonon replicas of NV^-. Although the spectral range of Raman setup used for measurements in this paper is limited by 650 nm, both the important ZPL lines are present in this range and the formulae $NV^0/(NV^0+NV^-)$ (see Fig. S2D) can be applied independently on the used setup.

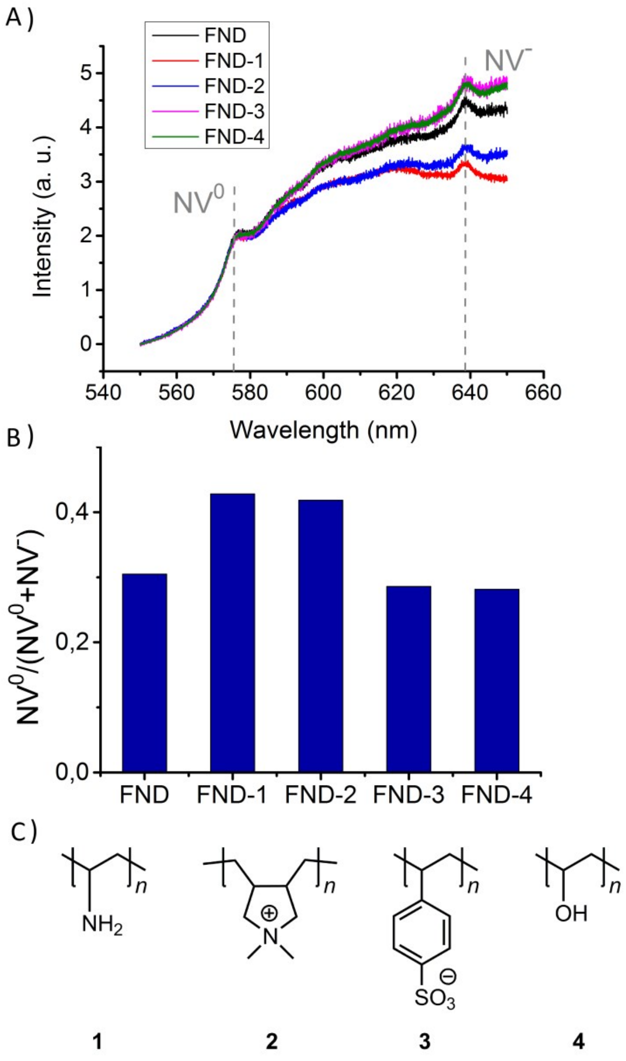

Figure S4: A) Section of fluorescence spectra involving ZPL of the NV^0 and NV^- states for FND and complexes with polymers **1-4** measured at pH ≈ 6. The spectra are normalized to the NV^0 ZPL. B) The relative changes in fluorescence expressed as $NV^0/(NV^0+NV^-)$ ratio from fluorescence data for FND-**1** and FND-**2** (cationic), FND-**3** (anionic), and FND-**4** (non-charged) complexes relative to unmodified FND. The ratios were calculated from maximum intensity of NV^0 and NV^- ZPL peaks in fluorescence spectra. C) The structures of poly(allylamine) (**1**), poly(diallyldimethylammonium) cation (**2**), poly(styrensulfonate) anion (**3**) and poly(vinylalcohol) (**4**). Note that polymers **2** (quartenary ammonium salt) and **3** (sulfonate) are inherently charged in aqueous solution, and their charges are not sensitive to pH changes.

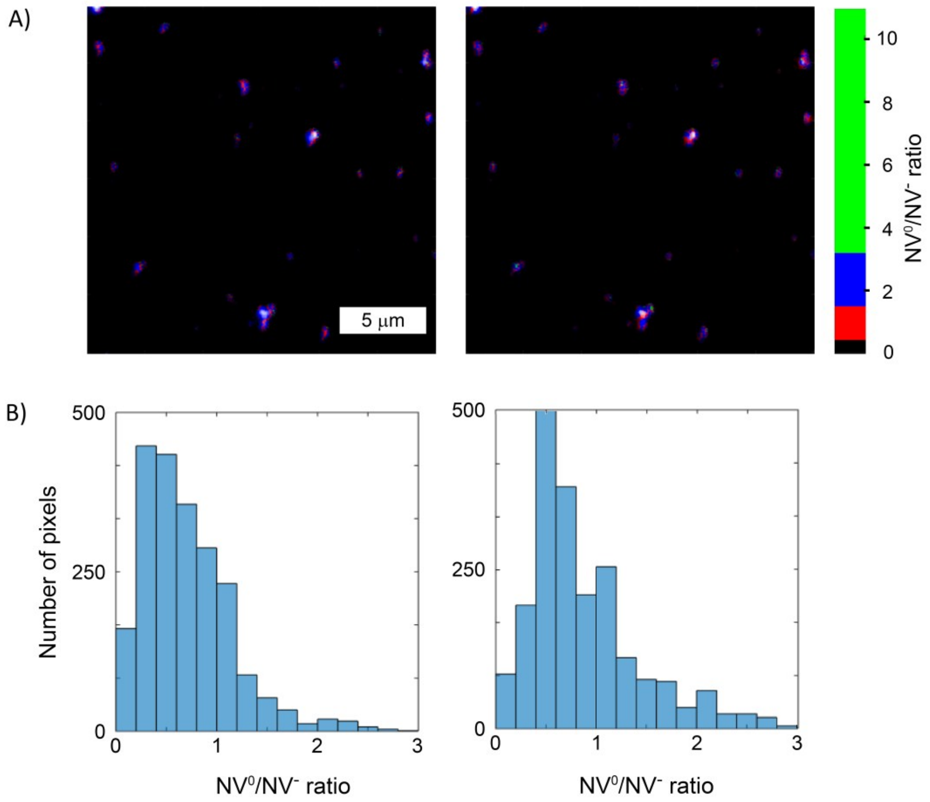

Figure S5: A) Fluorescence image showing NV^0/NV$^-$ ZPL fluorescence intensity ratio of FND particles deposited on glass slide covered in droplet of water (left) and of FND-**3** complex (right) formed 10 minutes after addition of **3**. C) Histogram representing the number of pixels per values of NV^0/NV$^-$ ZPL fluorescence intensity ratio for FND (left) and FND-**3** (right). Addition of anionic polymer **3** did not cause any significant changes either in images or in histograms. The total number of pixels was the same in both cases.